



## Optimisation of an electronic amplifier applied to electrolyte/insulator/semiconductor structure

Jérôme Launay, M.L. Pourciel-Gouzy, W. Sant, A. Martinez, Pierre Temple-Boyer

### ► To cite this version:

Jérôme Launay, M.L. Pourciel-Gouzy, W. Sant, A. Martinez, Pierre Temple-Boyer. Optimisation of an electronic amplifier applied to electrolyte/insulator/semiconductor structure. *Analytica Chimica Acta*, 2005, 545 (2), pp.195-199. 10.1016/j.aca.2005.04.079 . hal-02881774

**HAL Id: hal-02881774**

**<https://laas.hal.science/hal-02881774>**

Submitted on 2 Jul 2020

**HAL** is a multi-disciplinary open access archive for the deposit and dissemination of scientific research documents, whether they are published or not. The documents may come from teaching and research institutions in France or abroad, or from public or private research centers.

L'archive ouverte pluridisciplinaire **HAL**, est destinée au dépôt et à la diffusion de documents scientifiques de niveau recherche, publiés ou non, émanant des établissements d'enseignement et de recherche français ou étrangers, des laboratoires publics ou privés.

# Optimisation of an electronic amplifier applied to Electrolyte/insulator/Semiconductor structures

J. Launay, M.L. Pourciel, W. Sant, A. Martinez, P. Temple-Boyer

LAAS-CNRS, 7 av. du colonel Roche, 31077 Toulouse Cedex 4, FRANCE

## Abstract

This paper reports on the development of a MOSFET-based amplifier for the electrical characterisation of chemical field effect capacitors (ChemFEC) based on electrolyte/insulator/semiconductor (EIS) capacitive structures. Experimental demonstration is performed through the study of  $\text{SiO}_2/\text{Si}_3\text{N}_4$  ion sensitive field effect capacitor (ISFEC) sensors for pH measurement. This study deals with the amplification's properties according to the ISFEC and MOSFET electrical characteristics. Thus, the ISFEC transition from the accumulation to the inversion regime is shown to be responsible for a non-linear phenomenon. Nevertheless, thanks to a compromise between the ISFEC flat band voltage and the MOSFET threshold voltage, linear responses and high detection sensitivities are evidenced on the [2 – 12] pH range. Thus, the non-linear phenomenon observed in previous works is clarified. The detection structure evidences linear responses, which is an essential parameter for sensors. Finally, high detection sensitivities are obtained on a small pH range due to this non-linearity.

**Keywords:** ChemFEC microsensor, MOSFET amplifier, improved detection properties

## 1. Introduction

The development of chemical field effect capacitors (ChemFECs), also called electrolyte/insulator/semi-conductor (EIS) sensors [1], can bring solutions in order to detect biochemical or/and biological species in liquid media. Indeed, they are somewhat simpler than chemical field effect transistors (ChemFETs) and are suited for both potentiometric or/and impedimetric detection. In return, their use requires adapted characterisation techniques. Solutions have been found either by using standard capacitance – voltage C-V measurements [2] or by developing light-addressable potentiometric sensor (LAPS) [3, 4, 5].

Another solution has proposed the development of electronic amplifiers adapted to the ChemFEC characterisation. It has lead to the study of a ChemFEC/MOSFET amplifier [6]. Thus, theoretic calculations and simulations have shown the potentialities of this amplifier for improving the detection properties of field-effect chemical sensors, taking into account static and dynamic phenomena [7]. However, even if improved detection sensitivities have been evidenced experimentally for the pH measurement, results have still exhibited an unclear non-linear phenomenom [6].

This paper deals with the study of the ChemFEC/MOSFET amplifier and aims to explain the pH detection non linear phenomenom through the experimental comparison of different ChemFEC chemical sensors and of different metal/oxide/semiconductor field effect transistors (MOSFET).

## 2. Experimental

The pH-sensitive field-effect capacitors (pH-ISFECs) were fabricated on <100>-oriented, P-type (3-5  $\Omega\cdot\text{cm}$ ) silicon substrate. The ionosensitive gate was formed using a silicon nitride  $\text{Si}_3\text{N}_4$  layer deposited on top of a thermally grown silicon dioxide  $\text{SiO}_2$  layer (figure 1). Special attention was given for obtaining high capacitance values by increasing the

capacitor area. The chemical sensors were formed on a chip designed with a specific geometry (about 8 millimetres long, 2.6 millimetres wide and 0.5 millimetre thick) (figure 2). Finally, the pH-ISFEC chips were stuck on printed circuit thanks to an insulating epoxy glue. After wire bonding and coating, encapsulation was performed using a silicone, leaving the sensitive parts uncovered (figure 3). All in all, two different pH-ISFEC sensors were fabricated for comparison (table 1).

In the following, the pH-ISFECs will be modelled by the association of an equivalent capacitor  $C_{th}$  and a voltage source  $E_{th}$  (figure 4).  $E_{th}$  represents the potential drop in the electrolyte at the insulator/electrolyte interface. According to the Nernst law, it can be related to the solution hydrogen potential pH as following [8]:

$$E_{th} = s_0(pH_{pzc} - pH) \quad (1)$$

where  $pH_{pzc}$  is the pH at the point of zero charge, estimated around 4 for silicon nitride  $Si_3N_4$  [9, 10], and  $s_0$  is the ISFEC sensitivity to pH, experimentally estimated around 55 mV/pH.

In order to study the influence of the pH-ISFEC characteristics on the behaviour of the ChemFET/MOSFET amplifier, two different MOSFET transistors, i.e. PMOS and NMOS type (table 2) were studied. Thus, two amplifying structures have been realised in order to keep a positive bias on the pH-ISFEC capacitor (figures 5 and 6). In both cases, the MOSFET transistor was biased by a KEITHLEY 220 current source (bias current:  $I_0 = 50 \mu A$ ) and the drain-source voltage  $V_{DS}$  variations with time was recorded thanks to a Tektronics TDS 220 oscilloscope. For all characterisation experiments, source voltages were applied to the solution using a reference calomel electrode.

Test solutions were realised by diluting hydrochloric acid HCl and tetramethylammonium hydroxide (TMAH)  $N(CH_3)_4OH$  with pure water. Solution pH were estimated by a ORION 710A digital pH-meter with a precision of  $\pm 0.01$  pH unit after

calibration with three standard buffer solutions (pH = 4.01, 7.00 and 10.01). All the measurements were done at a constant temperature (20°C).

### 3. Comparison of the pH-ISFEC/MOSFET structures

The theoretic study of the ChemFEC/MOSFET amplifier has been described elsewhere [6]. Here will be only compared the PMOS and the NMOS amplifier applied to our capacitive sensor.

For the NMOS amplifier (figure 5), considering that the gate voltage  $V_G$  is constant and that the gate current  $I_G$  is negligible [6], the drain voltage  $V_D$  is given by:

$$\boxed{\phantom{V_D = V_G - \frac{1}{\beta_n} \left( \frac{1}{V_{thn}} - \frac{1}{V_G - V_{thn}} \right) \left( \frac{1}{V_D} - \frac{1}{V_G - V_{thn}} \right)}} \quad (2)$$

Since the drain voltage  $V_D$  is positive and taking into account equation (1), it can be written:

$$\boxed{\phantom{V_D = V_G - \frac{1}{\beta_n} \left( \frac{1}{V_{thn}} - \frac{1}{V_G - V_{thn}} \right) \left( \frac{1}{V_D} - \frac{1}{V_G - V_{thn}} \right)}} \quad (3)$$

For the PMOS amplifier (figure 6) and with the same assumptions than previously, the drain voltage  $V_D$  is given by:

$$\boxed{\phantom{V_D = V_G - \frac{1}{\beta_p} \left( \frac{1}{V_{thp}} - \frac{1}{V_G - V_{thp}} \right) \left( \frac{1}{V_D} - \frac{1}{V_G - V_{thp}} \right)}} \quad (4)$$

Since the drain voltage  $V_D$  is negative and always taking into account equation (1), it can be written:

$$\boxed{\phantom{V_D = V_G - \frac{1}{\beta_p} \left( \frac{1}{V_{thp}} - \frac{1}{V_G - V_{thp}} \right) \left( \frac{1}{V_D} - \frac{1}{V_G - V_{thp}} \right)}} \quad (5)$$

Therefore, from equations (3) and (5), the absolute value of the drain voltage  $\boxed{\phantom{V_D}}$  follows similar variations with pH whatever the amplifier type. This parameter will therefore be studied hereafter.

### 4. Results and discussion

Related to the previous study [6], variations of the voltage  $V_{\max}$  have been plotted as a function of solution pH for several capacitances  $C$  (figure 7). These results have been obtained with the ISFEC #1 (table 1) and the PMOS transistor (table 2).

Non-linear curves are evidenced whatever the value of  $C$  for a pH value around 4. In order to explain this non-linear phenomenon, different assumptions, either related to dynamic effects, either related to the chemical properties of the  $\text{Si}_3\text{N}_4$  ionosensitive film chemical properties, were proposed and discarded [6].

From another point of view, the non-linearity could be related to the ISFEC transition from the accumulation regime to the inversion one. Indeed, since the  $V_{\text{GS}}$  voltage is assumed to be constant, roughly equal to the MOSFET threshold voltage  $V_{\text{T}}$  [6], the variations of the pH value induce variations on the ISFEC voltage  $V$ .

Thanks to this last assumption and using the electric model of the pH-ISFEC (figure 4) and the PMOS amplifier (figure 6), the non-linear phenomenon observed on figure 7 allows an estimation of the ISFEC #1 flat-band voltage  $V_{\text{FB}}$ :

$$\boxed{\phantom{V_{\text{FB}} = V_{\text{T}} - \frac{qN_{\text{A}}}{C_{\text{ox}}}}} \quad (6)$$

else:  $\boxed{\phantom{V_{\text{FB}} = V_{\text{T}} - \frac{qN_{\text{A}}}{C_{\text{ox}}}}}$

We therefore obtain a good agreement with the flat-band voltage value determined using quasi-static capacitance-voltage  $C(V)$  experiments on the ISFEC#1 capacitor (Table 1).

To complete the study, the ISFEC #1 has been studied using the NMOS amplifier (figure 5) with the corresponding NMOS transistor (table 2). In this case, linear curves are therefore observed on the [2 - 12] pH range (figure 8). In fact, if the non-linear phenomenon is related to the ISFEC accumulation - inversion transition, a simple calculation gives the pH value where it should appear:

$$\boxed{\phantom{pH = 4}} \quad (7)$$

else:  $\boxed{\phantom{pH = 4}}$

The second generation of ISFEC sensors allows checking again the influence of the ISFEC accumulation - inversion transition. Figure 9 shows the NMOS amplifier output characteristics using an ISFEC#2 sensor (table 1). Again, non-linear phenomena are evidenced, this time around  $\text{pH} = 8.5$ . Firstly, this pH shift between figures 7 and 9 demonstrates definitively that the non-linearity is not related to  $\text{pH}_{\text{PZC}}$  value [6]. Secondly, this result should allow to determine the ISFEC#2 flat-band voltage  $V_{\text{FB}}$ :

Again, a good agreement is obtained with the flat-band voltage value determined using quasi-static capacitance-voltage  $C(V)$  experiments on the ISFEC#2 capacitor (Table 1).

$$\text{else: } \boxed{\phantom{\text{code}}} \tag{7}$$

## 5. Conclusions

MOSFET-based amplifier symmetry have been studied whatever the MOS transistor type. The non-linear phenomenon evidenced in some case has been related to the ISFEC transition from the accumulation to the inversion regime. This effect has been tackled off by

choosing in an optimal way the MOSFET threshold voltage and, thus, by discarding the ISFEC flat-band voltage value from the ISFEC voltage range on the [2 - 12] pH range (equation 1). Therefore, whatever the ISFEC tested, a compromise on the amplifier will be always possible in order to reach linear responses and high detection sensitivities.

Nevertheless, non-linear effects could be interesting for any applications working on small pH ranges such as medical ones. Indeed, zooming on figure 9, the non-linear phenomenon offers a very high sensitivity (3.5 V/pH) for pH around 8. Furthermore, as the non-linearity is due to the capacitive structure, sensitivity could be still increased by modifying the doping profile of ISFEC sensors. Thus, by adjusting the compromise between the MOSFET type and the ISFEC flat-band voltage, it should be possible to obtain an optimal sensitivity on specific detection range.

## References

- [1] D.R. Thévenot, K. Toth, R.A. Durst, "Electrochemical biosensors: recommended definitions and classification", *Biosensors & Bioelectronics*, 16 (2001), 121-131
- [2] F. Chauvet, A. Amari, A. Martinez: "Stability of silicon nitride/silicon dioxide/silicon electrodes used in pH microelectronic sensors", *Sensors and Actuators*, Vol.6 (1984), 255
- [3] D. Hafeman, J. Parce, H. McConnell: "Light-addressable potentiometric sensor for biochemical systems", *Science*, 240 (1988), 1182-1185
- [4] A. Ismail, H. Sugihara, T. Yoshinobu, H. Iwasaki: "A novel low-noise measurement principle for LAPS and its application to faster measurement of pH", *Sensors and Actuators*, B 74 (2001), 112-116
- [5] G. Ferri, P. De Laurentiis, A. D'Amico, C. Di Natale: "A low-voltage integrated CMOS analog lock-in amplifier prototype for LAPS applications", *Sensors and Actuators*, A 92 (2001), 263-272



- [6] P. Temple-Boyer, J. Launay, G. Sarraeyrouse, A. Martinez: "Study of capacitive structures for amplifying the sensitivity of FET-based chemical sensors", *Sensors and Actuators*, B78 (2001), 285-290
- [7] P. Temple-Boyer, J. Launay, G. Sarraeyrouse, A. Martinez: "Amplifying structure for the development of field effect capacitive sensors", *Sensors and Actuators*, B4318 (2002), 1-11
- [8] L. Bousse, N.F. De Rooij, P. Bergveld: "Operation of chemically sensitive field effect sensors as a function of the insulator-electrolyte interface", *IEEE Transactions on Electron Devices*, ED30 (1983), 1263
- [9] M. Grattarola, G. Massobrio, S. Martinoia: "Modeling  $H^+$ -sensitive FET's with SPICE", *IEEE Transactions on Electron Devices*, ED39 (1992), 813
- [10] A.A. Pogossian: "Determination of the pH<sub>pzc</sub> of insulators surface from capacitance-voltage characteristics of MIS and EIS structure", *Sensors and Actuators*, B 44 (1997), 551-553

## **Biographies**

Jérôme Launay was born the 11<sup>th</sup> of March 1975. He received the degree in electronic engineering and his Diplôme d'Etudes Approfondies in Microelectronics from the Institut National des Sciences Appliquées de Toulouse (France) in 1998. He joined the Laboratoire d'Architecture et d'Analyse des Systèmes from the french Centre National de la Recherche Scientifique (LAAS-CNRS) in 1998. His research activities includes development of CHEMFETs chemical sensors for medical applications.

Marie-Laure Pourciel was born the 25<sup>th</sup> of July 1976. She received her master in Physics degree from the Université Paul Sabatier de Toulouse (France) in 1999 and her Diplome d'Etudes Approfondies in Biotechnology from the Institut National des Sciences Appliquées de Toulouse (France) in 2000. She joined the Laboratoire d'Architecture et d'Analyse des

Systèmes from the French Centre National de la Recherche Scientifique (LAAS-CNRS) in 2000. She is preparing a PhD thesis on the development of chemical microsensors for biochemical applications.

William Sant was born the 18<sup>th</sup> of May 1969. He received his master in electronics degree in 1996 and his Diplome d'Etudes Approfondies in Microelectronics from the Université Paul Sabatier de Toulouse (France) in 1999. He joined the Laboratoire d'Architecture et d'Analyse des Systèmes from the French Centre National de la Recherche Scientifique (LAAS-CNRS) in 2000. He is preparing a PhD thesis on the development of chemical microsensors for medical applications.

Augustin Martinez was born the 24<sup>th</sup> of May 1942. He joined the Laboratoire d'Architecture et d'Analyse des Systèmes from the french Centre National de la Recherche Scientifique (LAAS-CNRS) in 1966 and received his Doctorat d'Etat ès Sciences Physiques from the university of Toulouse (France) in 1976. In 1980, he became Professor at the Institut National des Sciences Appliquées de Toulouse. He has been in charge of the Microstructures et Microsystèmes intégrés group since 1992 and is assistant director for the LAAS-CNRS since 1997.

Pierre Temple-Boyer was born the 25<sup>th</sup> of October 1966. He received the degree in electronic engineering from the Ecole Supérieure d'Electricité (Paris – France) in 1990. He joined the Laboratoire d'Architecture et d'Analyse des Systèmes from the french Centre National de la Recherche Scientifique (LAAS-CNRS) in 1992 and received the PhD degree from the Institut National des Sciences Appliquées de Toulouse (France) in 1995. Since then, as a senior researcher, he has been working on the development of micro- and nanotechnologies.

## FIGURE CAPTIONS

Figure 1: structure of the pH-ISFEC

Figure 2: picture of the pH-ISFEC silicon chip

Figure 3: silicone encapsulation

Figure 4: electric model of the pH-ISFEC

Figure 5: schematic of the NMOS amplifier

Figure 6: schematic of the PMOS amplifier

Figure 7: voltage  $V_{\max}$  as a function of solution pH for different capacitances  $C$

$$(C_{\text{th}} = 1.9 \text{ nF} / V_T = -1.4\text{V})$$

Figure 8: voltage  $V_{\max}$  as a function of solution pH for different capacitances  $C$

$$(C_{\text{th}} = 1.9 \text{ nF} / V_T = 0.8\text{V})$$

Figure 9: voltage  $V_{\max}$  as a function of solution pH for different capacitances  $C$

$$(C_{\text{th}} = 1.5 \text{ nF} / V_T = 0.8\text{V})$$

Figure 10: voltage  $V_{\max}$  as a function of solution pH for different capacitances  $C$

$$(C_{\text{th}} = 1.5 \text{ nF} / V_T = -1.4\text{V})$$

Figure 11: amplification ratio  $r$  as a function of the capacitance ratio  $C_{\text{TH}}/(C+C_{\text{GD}})$

Figure 12: high sensibility due to thenon-linear phenomenon

Table 1: ISFEC characteristics

Table 2: MOSFET characteristics

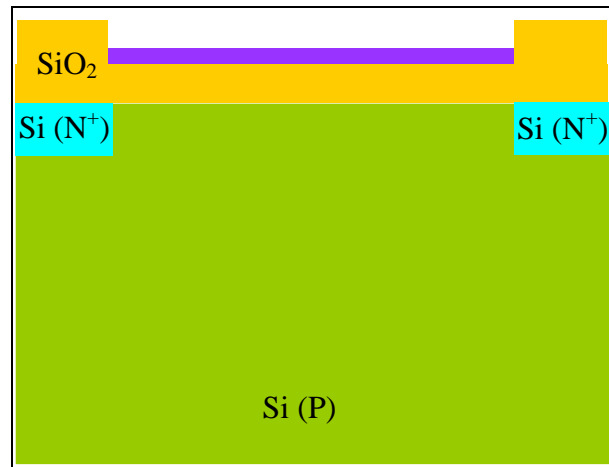


Figure 1: structure of the pH-ISFEC

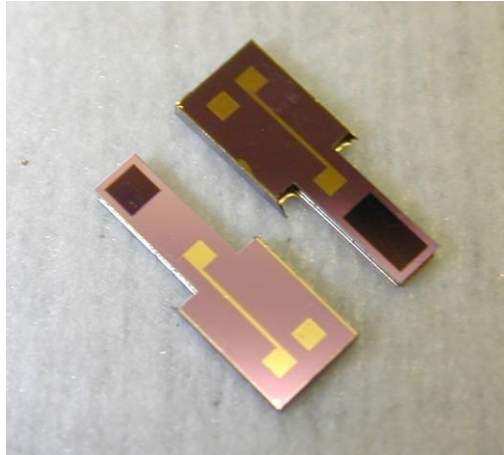


Figure 2: picture of the pH-ISFEC silicon chips

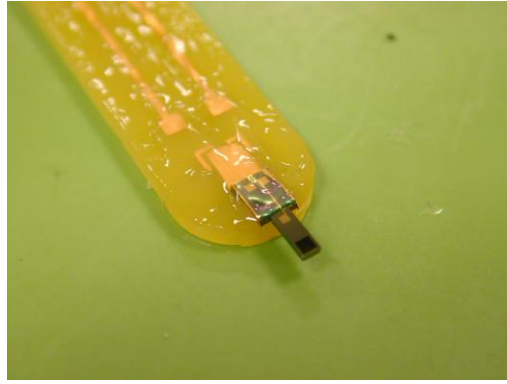


Figure 3: silicone encapsulation of the pH-ISFECs



Figure 4: electrical model of the pH-ISFEC





Figure 5: schematic of the NMOS amplifier



Figure 6: schematic of the PMOS amplifier

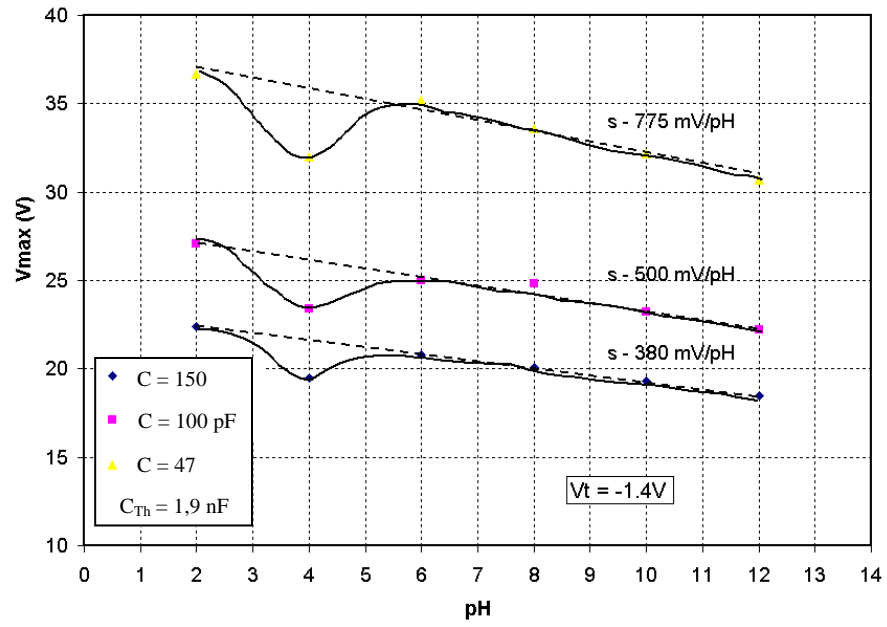


Figure 7: voltage  $V_{\max}$  as a function of solution pH for different capacitances  $C$   
 $(C_{\text{th}} = 1.9 \text{ nF} / V_T = -1.4 \text{ V})$

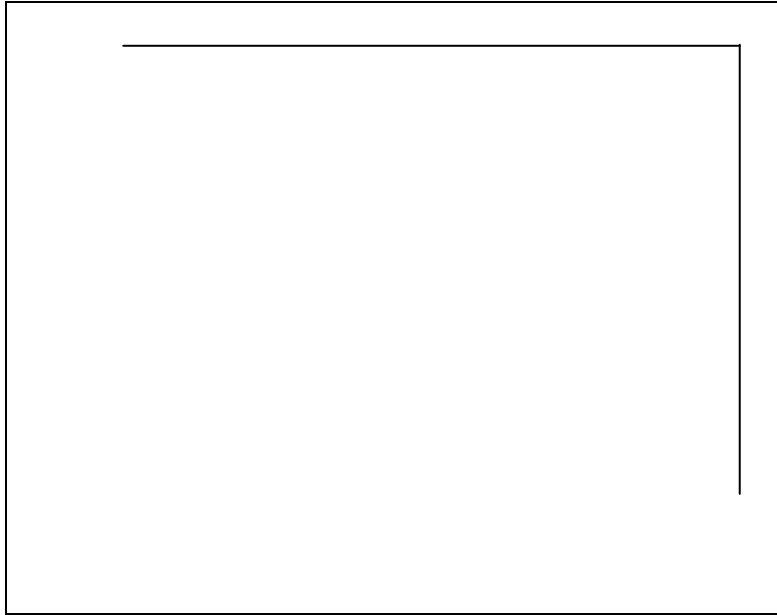


Figure 8: voltage  $V_{\max}$  as a function of solution pH for different capacitances  $C$

$$(C_{\text{th}} = 1,9 \text{ nF} / V_{\text{T}} = 0,8\text{V})$$

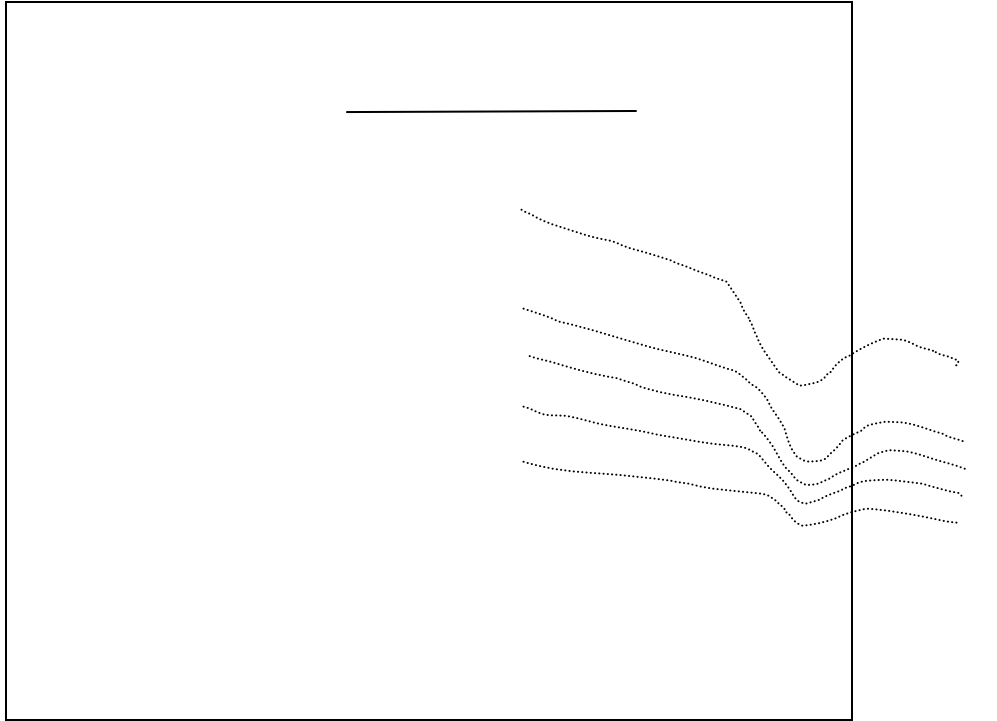


Figure 9: voltage  $V_{\max}$  as a function of solution pH for different capacitances  $C$

$$(C_{\text{th}} = 1,5 \text{ nF} / V_T = 0,8\text{V})$$



Figure 10: voltage  $V_{\max}$  as a function of solution pH for different capacitances  $C$   
( $C_{\text{th}} = 1,5 \text{ nF}$  /  $V_T = -1,4\text{V}$ )

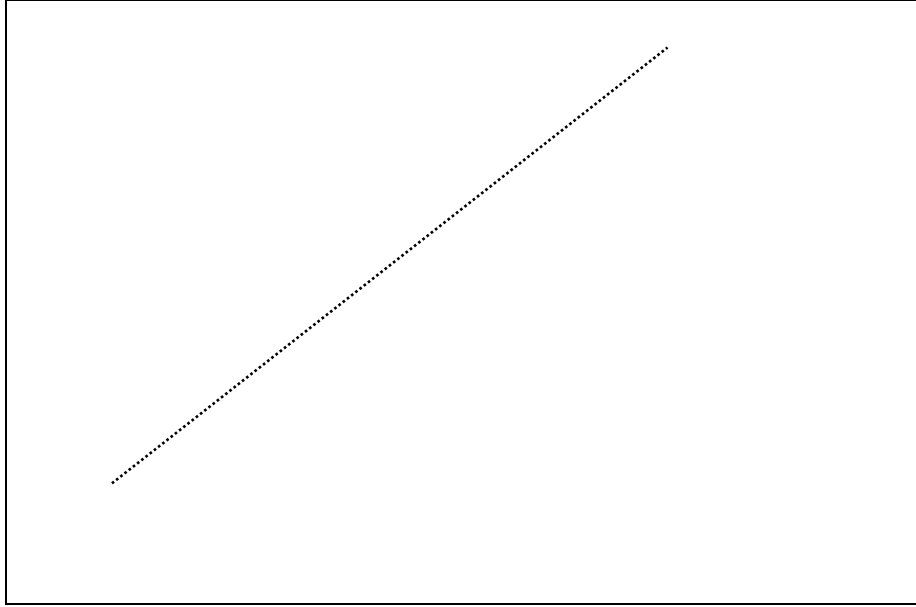


Figure 11: amplification ratio  $r$  as a function of the capacitance ratio  $C_{th}/(C+C_{GD})$

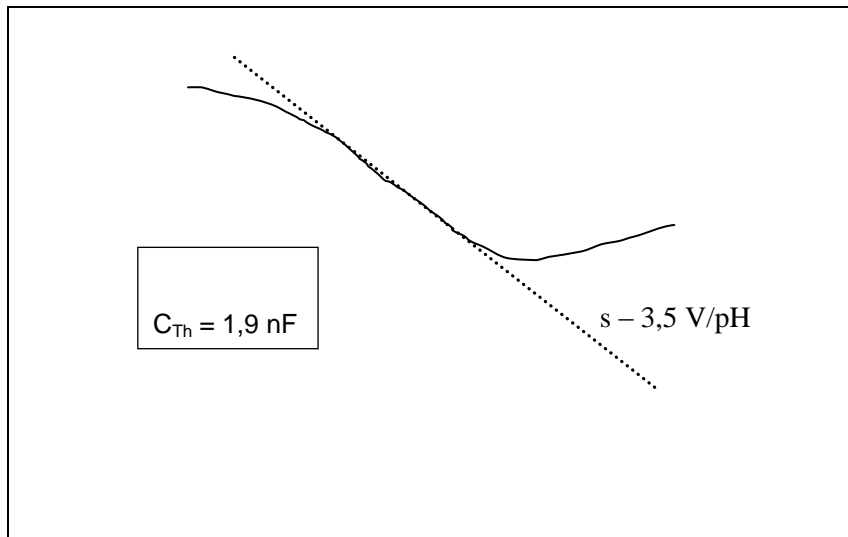


Figure 12: high sensibility due to the non-linear phenomenon



ISFEC type	Gate structure	Gate surface	Gate capacitance	Flat-band voltage $V_{FB}$
# 1	$\text{SiO}_2 / \text{Si}_3\text{N}_4$ (50nm / 50nm)	$4 \text{ mm}^2$	1.9 nF	$\approx 1.2 \text{ V}$
# 2	$\text{SiO}_2 / \text{Si}_3\text{N}_4$ (30nm / 30nm)	$2 \text{ mm}^2$	1.5 nF	$\approx 0.4 \text{ V}$

Table 1: ISFEC electrical characteristics

MOSFET type	Threshold voltage $V_T$ (V)	Drain-Source capacitance $C_{GD}$
PMOS	- 1.4 V	40 pF
NMOS	+ 0.8 V	25 pF

Table 2: MOSFET electrical characteristics